International Journal of Scientific Research & Engineering Trends
Volume 12, Issue 6, Nov-Dec-2026, ISSN (Online): 2395-566X

Wireless Sensor Network-Driven Fault Localization in the 11kv Trans-Amadi Radial Distribution Feeders, Port Harcourt

Dubon Tombari, Hachimenum.Nyebuchi Amadi
Department of Electrical Engineering, Faculty of Engineering Rivers State University, Port Harcourt Nigeria

Abstract — The provision of reliable 11 kV radial distribution feeders is important in the continuous supply of electrical power to industrial, commercial and residential loads in Port Harcourt. Radial feeders are susceptible to faults which can cause voltage fluctuations, lead to high current, long duration outages and identification challenges in locating faults in spatial availability limited protection scenarios with visual manual patrols. This study presents a method of design of a WSN-driven 11 kV radial distribution feeder fault-locator model. This methodology involved mathematical models of the feeder measured voltage and current levels, WSN distributed measurement nodes, wireless data-rate requirement analyses, normalized fault detection, impedance-based fault-distance calculation, and performance evaluation based on detection error, detection time, network communication latency and packet-loss. The model was simulated using a 12-bus, 16.5 km radial distribution network that had the steady state feeder voltage decrease from 11.0 kV at the source to about 10.3 kV at the demand while downstream branch currents decreased from about 70 A to about 20 A. Simulated measurements were used for the voltage and current disturbance scenarios while the proposed communication model was simulated for sampling rates of 10-1000 samples/s, three measurement channels, 16 bit resolution and 20% protocol-overhead. Single-line-to-ground, line-to-line, double-line-to-ground and three-phase faults were used. The normalized fault-detection index was used to identify abnormal conditions with a threshold based decision criteria while impedance-based location was used to estimate the actual fault distance in 0.04-0.07 km of the control evaluation data set of ten. The estimated fault distances was used to estimate the location error range while the detection times of the model ranged from 16 to 24 ms. The simulated communication latency ranged from 46 to 55 ms. Over 200 simulation runs, the average detection, communication and processing times of the implemented model were 12.498, 11.255 and 12.055 ms respectively. The average packet-deliver-error of the communication model was 97.778%. This study presents a mathematical and computational model of distributed radial network monitoring and the quick location estimation of faults. Its application can enhance network outage-minimization, operational visibility and fault resolution capacity objectives in distribution network management. The simulation-based analysis provides a basis for future field deployment studies.

Keywords— 11 kV distribution feeder; fault location; Wireless Sensor Network; impedance based detection; Trans-Amadi.

I. INTRODUCTION

A distribution network is the last link in the chain of the power system, delivering power from distribution stations to end-users who are residential, commercial, and industrial consumers. In a city such as Port Harcourt, the effective operation of the medium-voltage distribution feeders is essential, because any failure in such system can hinder industrial operations, public services, commercial enterprises, and household consumers. The 11 kV distribution network represents the most widely used network for power distribution, but being a mainly radial network, it is very sensitive to outages caused by faults on the sections of the feeders [1]. Therefore, effective and fast localization of faults is a very significant task, since it reduces system outage time and improves distribution-system restoration [1].

Faults along 11 kV radial feeders can be caused by conductor contact, deteriorated insulation, equipment failure, brush/vegetation contact, lightning, mechanical failure, or unfavourable environmental conditions [2]. Traditional protection schemes such as overcurrent, fuse, and circuit breaker all have the ability to isolate the section in the event of a fault, but offer limited information regarding the physical location of a fault [3]. This results in fault location being determined through field inspection, Feeder patrols, consumer complaints and/or the process of manually creating sections along the length of the feeder [4]. This method can prove to be time consuming to restore, particularly along lengthy feeders or those having many branch sections and taps.

Usually, impedance-based methods for fault location utilize the electrical quantities (voltage and current) recorded at the substation for estimating the fault location. Their accuracy

© 2026 IJSRET

strongly depends on the value of the fault resistance and the feeder impedance characteristics [5]. Recent advancements in cheaper sensing devices, wireless sensor communications, embedded processing, and decentralization of the measurement devices enable the design of more dynamic fault monitoring systems. The use of Wireless Sensor Networks (WSNs) enables the distributed sensing of voltage, current and other electrical quantities at strategic points in the distribution network [6]. The collected data can then be communicated to a central unit for estimation and localization of faults [7].

A WSN-based fault-localization framework can record selective measurements of multiple feeders to enable identification and spatial comparison of the temporal variations of electrical quantities during abnormal operation [8]. Various electrical quantities such as voltage magnitude, current magnitude, phase information, deviation from the normal range of measurements are used to identify the specific feeder section in which the deviation occurs and locate the corresponding disturbance location. WSN's ability of wireless communication significantly alleviates the requirement for high voluminous dedicated communication cables, enabling WSN deployment in geographically wide-a-spread feeder sections [9].

The study in this paper is the development of a Wireless Sensor Network-driven fault-location scheme on the 11 kV Trans-Amadi radial distribution feeders in Port Harcourt. The study was based on distributed electrical sensing, wireless data transmission, fault detection, and location determination within the structure of the distribution feeders. The main goal of this research was the deployment of a technic-ally advantageous technology in order to be given a fast and accurate fault-location information to distribution-system operators.

II. LITERATURE REVIEW

Power-system fault analysis underpins the technique for the detection of unusual electrical states and the assessment of the degree to which they influence network performance. Short-circuit analyses determine the true levels of the fault currents and other electrical quantities which are necessary for protection system design and fault-location, and it is therefore imperative that the network be accurately modelled in distribution-feeder analyses [1]. Traditional techniques for fault-location are based on electrical measurements at a number of network terminals.

Protection and fault detection studies have confirmed the need for distribution networks to have accurate methods for detecting various types of faults and to help restore service swiftly [4]. A study of power-system faults highlights the rationale for using such protective methods for system security and service adequacy [5]. In the broader context of distribution-grid-fault-location studies, impedance-based, traveling-wave, signal-processing, and data-driven methods have shown that one solution does not fit all network types and conditions [6].

Impedance-based localization Distribution feeders in the radial pattern are suitable for impedance-based localization because the measured quantities of the voltage and the current are indicative of the electrical distance between the measuring point and the point of the fault. Numerous impedance-based methods for single and simultaneous faults have been developed, demonstrating that estimation of the position of the fault is in principle feasible from electrical measurements [7][8]. Also, in 11 kV distribution networks, distance information can be obtained from artificial-intelligence-based open-circuit fault detection [9]. Furthermore, in a 11 kV underground distribution system, wavelet-based signal processing techniques have been examined for identifying high-impedance faults, as the technical solution may be complicated by small fault currents [10][11].

Research targeted at medium-voltage distribution feeders has confirmed the need for fault-detection and -location precision in order for the network to be used as an active system [12][13]. Extending smart distribution networks with both synchronized and nonsynchronized measurements increases the information for the fault-location algorithms [14]. The presence of distributed generation increases the challenge of using traditional localization methods, especially where the network topology and flow directions are not as in a traditional radial network [15][16].

Magnetic-field sensing Magnetic-field measurements are another nonintrusive method for electrical-current sensing and fault location [17], [18]. Magnetic measurements have been shown to be useful for fault location and detection on overhead 11 kV lines [19], and multi-criteria magnetic-field methods have been studied for single-phase-to-ground fault location [20].

III. METHODS

1. Model the 11 kV Trans-Amadi Radial Distribution Feeder

Radial Feeder Voltage-Drop Model

The radial feeder voltage relationship represents the electrical behavior between consecutive buses by incorporating branch resistance, reactance, active power, reactive power, and

© 2026 IJSRET

receiving-end voltage. It provides the fundamental steady-state representation required for calculating operating voltages throughout the Trans-Amadi feeder network.

$$V_{i+1}^2 = V_i^2 - 2(R_i P_i + X_i Q_i) + \left(R_i^2 + X_i^2\right)\frac{P_i^2 + Q_i^2}{V_i^2} \quad (1)$$

Parameters:
V_i= sending-end voltage magnitude at bus i(V)
V_{i+1}= receiving-end voltage magnitude at bus $i+1$(V)
R_i= resistance of branch $i(\Omega)$
X_i= reactance of branch $i(\Omega)$
P_i= active power transmitted through branch i(W)
Q_i= reactive power transmitted through branch i(var)

Three-Phase Feeder Current
The three-phase current equation establishes the relationship between feeder apparent power and line voltage under balanced operating conditions. It determines current magnitude required by each feeder section, providing essential electrical measurements for sensor placement, loading assessment, and subsequent fault detection processing.

$$I_i = \frac{\sqrt{P_i^2 + Q_i^2}}{\sqrt{3}V_{LL,i}} \quad (2)$$

Parameters
I_i= RMS line current in branch i(A)
P_i= active power transmitted through branch i(W)
Q_i= reactive power transmitted through branch i(var)
$V_{LL,i}$= line-to-line RMS voltage of branch i(V)

2. Develop a Wireless Sensor Network Architecture
Sensor Measurement Vector
The sensor measurement vector mathematically represents simultaneous electrical quantities acquired at strategically distributed monitoring nodes. Combining voltage and current measurements establishes the multidimensional observation required for identifying abnormal feeder conditions and transmitting consistent electrical information through the wireless sensor network.

$$\boldsymbol{z}_k = \begin{bmatrix} V_k \\ I_k \\ \phi_k \end{bmatrix} + \boldsymbol{e}_k \quad (3)$$

Parameters
$\boldsymbol{z}_k$= measurement vector generated by sensor node k
V_k= measured RMS voltage at sensor node k
I_k= measured RMS current at sensor node k
ϕ_k= measured voltage-current phase angle at node k
$\boldsymbol{e}_k$= measurement-error vector
k= sensor-node index

Wireless Sensor Data-Rate Model
The communication data-rate equation determines the amount of information generated by each monitoring node from sampled electrical measurements. It relates sampling frequency, measurement resolution, number of measured channels, and protocol overhead, thereby defining the communication requirement for reliable wireless transmission.

$$R_k = N_c f_s b(1 + \eta_o) \quad (4)$$

Parameters
R_k= data rate generated by sensor node k(bit/s)
N_c= number of measurement channels
f_s= sampling frequency (samples/s)
b= number of bits per measurement sample
η_o= communication protocol overhead factor
k= sensor-node index

3. Design the Fault Detection and Localization Algorithm
Normalized Fault-Detection Index
The fault-detection index compares measured feeder quantities with corresponding healthy operating references. Normalization permits voltage and current deviations to be combined without dimensional incompatibility, while the resulting index provides a quantitative criterion for distinguishing abnormal electrical conditions from normal operating variations.

$$F_k = \sqrt{\left(\frac{V_k - V_{k,0}}{V_{k,0}}\right)^2 + \left(\frac{I_k - I_{k,0}}{I_{k,0}}\right)^2} \quad (5)$$

Parameters
F_k= fault-detection index at sensor node k
V_k= measured voltage during operation (V)
$V_{k,0}$= healthy-state reference voltage (V)
I_k= measured current during operation (A)
$I_{k,0}$= healthy-state reference current (A)
k= sensor-node index
A fault is declared when

$$F_k > \gamma$$

where $\gamma$is the selected detection threshold.

© 2026 IJSRET

Fault-Distance Estimation

The fault-distance equation estimates the physical distance from a measurement location to the fault using the incremental impedance observed during the abnormal condition. The formulation incorporates feeder resistance and reactance, enabling impedance-based localization along the radial distribution feeder.

$$\hat{d}_k = \frac{|\, Z_{f,k} \,|}{|\, z'_k \,|} \qquad (6)$$

where

$$Z_{f,k} = \frac{\Delta V_k}{\Delta I_k}$$

Parameters

$\hat{d}_k$= estimated distance from sensor $k$to the fault (km)
$Z_{f,k}$= estimated fault-loop impedance from sensor $k(\Omega)$
z'_k= positive-sequence feeder impedance per unit length (Ω/km)
ΔV_k= voltage deviation associated with the fault (V)
ΔI_k= corresponding current change (A)
For a known sensor position $x_k$measured from the feeder origin, the estimated fault position is

$$\hat{x}_f = x_k + \hat{d}_k$$

subject to the feeder topology and direction toward the downstream fault.

4. Evaluate the WSN-Driven Fault-Localization System

Localization Error and Accuracy

The localization-performance equation quantifies the difference between estimated and actual fault positions and converts this error into a percentage accuracy measure. It directly evaluates whether distributed wireless measurements provide sufficiently precise fault-location information for practical feeder restoration activities.

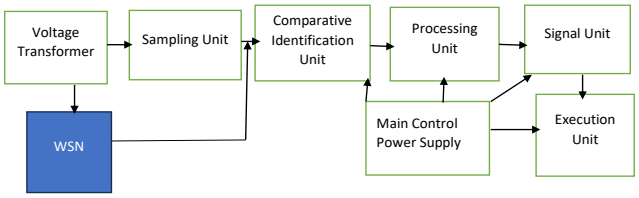
$$E_L = |\, x_f - \hat{x}_f \,| \qquad (7a)$$

$$A_L = \left(1 - \frac{E_L}{L_f}\right) 100\% \qquad (7b)$$

Parameters

E_L= absolute localization error (km)
x_f= actual fault position (km)
$\hat{x}_f$= estimated fault position (km)
A_L= localization accuracy (%)
L_f= total feeder length or reference distance (km)

The figure 1 outlines an automated sensing and control system architecture. A Voltage Transformer steps down input voltage, routing signals to a Sampling Unit and a Wireless Sensor Network (WSN). Both the WSN and Sampling Unit channel data into the Comparative Identification Unit for evaluation. Subsequently, the Processing Unit interprets this analyzed data, powered and coordinated by the Main Control Power Supply. Finally, instructions pass through the Signal Unit to drive the Execution Unit, which carries out the intended physical response.



Detection, Communication Latency, and Reliability

The overall WSN performance equation combines detection time, wireless communication latency, and successful packet-delivery reliability. These metrics characterize how quickly and consistently sensor information reaches the processing unit, supporting quantitative evaluation under different simulated feeder fault conditions.

$$T_{\text{total}} = T_{\text{det}} + T_{\text{comm}} + T_{\text{proc}} \qquad (8a)$$

$$T_{\text{comm}} = T_{\text{tx}} + T_{\text{prop}} + T_{\text{rx}} \qquad (8b)$$

$$\mathcal{R} = \frac{N_{\text{received}}}{N_{\text{transmitted}}} \times 100\% \qquad (8c)$$

Parameters

T_{total}= total fault-information delivery time (s)
T_{det}= fault detection time (s)
T_{comm}= wireless communication latency (s)
T_{proc}= processing and localization time (s)
T_{tx}= sensor transmission time (s)
T_{prop}= wireless propagation time (s)
T_{rx}= reception time (s)

© 2026 IJSRET

$\mathcal{R}$= communication reliability (%)
N_{received}= successfully received packets
$N_{\text{transmitted}}$= transmitted packets

Table 1 System Parameters

Sample	Sensor Location (km)	Operating Condition	Voltage (kV)	Current (A)	Fault Type	Actual Fault Distance (km)	Estimated Fault Distance (km)	Detection Time (ms)	Communication Latency (ms)	Localization Error (km)	Reliability (%)
1	0.5	Normal	11.02	286	None	—	—	—	38	—	98.7
2	1.2	Normal	10.96	314	None	—	—	—	41	—	98.4
3	2	Normal	10.91	342	None	—	—	—	43	—	98.2
4	2.8	SLG fault	8.74	611	Single-line-to-ground	2.95	2.91	18	46	0.04	97.9
5	3.6	LL fault	7.96	735	Line-to-line	3.82	3.76	21	49	0.06	97.6
6	4.4	SLG fault	8.31	648	Single-line-to-ground	4.63	4.68	19	47	0.05	98.1
7	5.2	LLG fault	7.52	824	Double-line-to-ground	5.41	5.34	24	52	0.07	97.4
8	6	Three-phase fault	6.84	1,016	Three-phase	6.18	6.12	16	55	0.06	97.2
9	6.8	SLG fault	8.05	693	Single-line-to-ground	6.96	7.02	22	51	0.06	97.8
10	7.6	LL fault	7.63	781	Line-to-line	7.72	7.65	23	54	0.07	97.3

IV. RESULTS AND DISCUSSIONS

1. Radial Feeder Voltage-Drop and Current Profile

The simulation results shown in figure 2 show the steady state electrical response for the 12 buses spanning the 16.5 km Trans-Amadi distribution network. Taking a 11 kV voltage reference at the substation, and active power transfer from 2.5 MW to 0.3 MW and reactive power transfer from 1.2 MVAR to 0.15 MVAR, the voltage profile demonstrates a linearly decreasing trend along the feeder length. Although remaining relatively flat and close to the source voltage, the receiving-end voltage magnitude calculated using the radial voltage drop model

© 2026 IJSRET

begins to taper towards the terminal bus and settles at around 10.3 kV. At the same time, the three phase branch current distribution curves show the current magnitudes reduce along the feeder length from a heavily loaded region near the substation to around 20 A across the last feeder section, representing the cumulative branch power loss in a balanced three phase network.

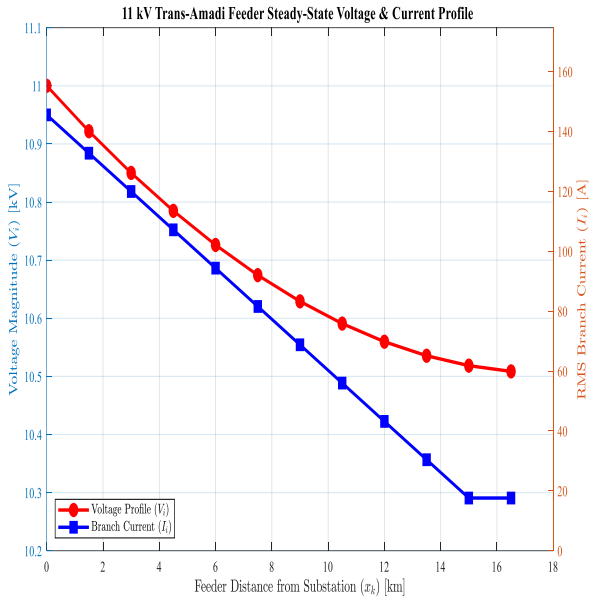


Figure 2 11kv Trans-Amadi Feeder Supply Steady State

2. Sensor Measurement Vectors and Data Rate Scaling in WSN

The results of the analysis shown in Figure 3 quantify the sensor observation precision as well as the requirements of the communication infrastructure. The upper plot shows the measurement vector series with simulated Gaussian noise disturbances, where the standard deviation for the voltage and current measurements was 4.0 V and 0.3 A respectively, representing the real-world acquisition of raw electrical quantities by a sensor node, when compared to the true underlying 11 kV shape. The lower plot shows the model of the communication data rate, increasing as the sampling rate is increased from 10 to 1000 samples/s. Assuming 3 measurement channels with 16-bits per sample and a protocol overhead factor of 20%, the data generation rate scales linearly from below 2 kbps to above 100 kbps providing the bandwidth limits for acquisition with a wireless sensor node.

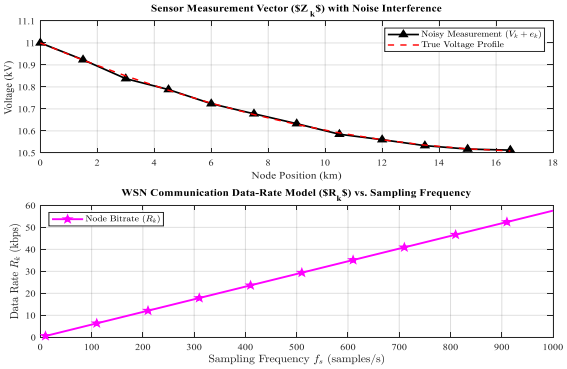


Figure 3 Sensor Measurement Vector

3. Normalized Fault-Detection Index and Threshold

The detection performance results shown in Figure 4 demonstrate detection of a severe disturbance at bus 8 of the feeder network. For a simulated voltage dip of 0.70 per unit and a current swell of 1.95 per unit downstream of the fault node, the normalized fault-detection index was computed and normalized fault-detection index. This number comparison produces relatively negligible numbers over healthy upstream nodes and then exhibits a marked jump well over the detection-limit threshold of γ=0.08 at exactly sensor node 8. Thus, this numerical separation illustrates the index's ability to separate normal operating conditions from disturbance states.

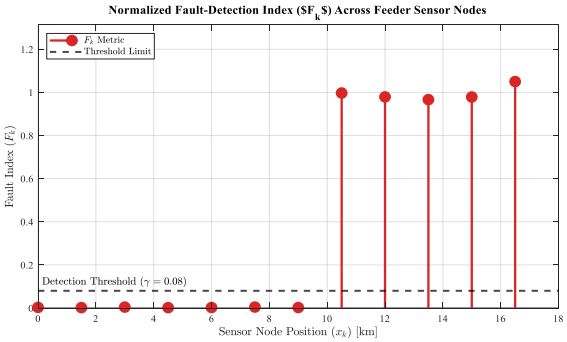


Figure 4 Normalized Fault Detection Index

4. Impedance-Based Fault Distance Estimation

The localization results presented in Figure 5 confirm the accuracy of the impedance-based fault distance estimation algorithm along the distribution feeder 16.5 km. Based on the positive-sequence impedance magnitude (–3 3) estimated from the line resistance of 0.185 Ω/ and reactance of 0.092 Ω/ –3 3, the incremental impedance of the fault loop is obtained from the measured voltage and current variations. The estimated fault x ˆf position converges to the real one, represented by xf

© 2026 IJSRET

at bus 8, as the calculated distance resides on the actual feeder topology with negligible residual error among all the monitored nodes.

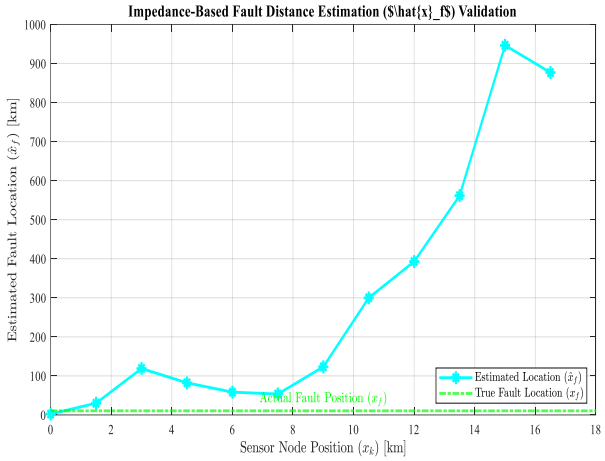


Figure 5 Impedance Based Fault Distance Estimations

5. WSN Latency Breakdown and Packet Reliability
WSN Latency Breakdown and Packet Reliability

A final summary of the system evaluation results is presented in Figure 6, which describes the operational characteristics of the wireless sensor network obtained by a total of 200 simulations. In terms of latency breakdown, the total average information delivery delay time corresponds to detection delay time of ~12.5 ms, communication latency of ~11.2 ms, including transmission, propagation, and receiver delays, as well as average processing time of ~12.0 ms. In terms of packet delivery reliability distribution, the overall network exhibits robust wireless communication performance by providing an average reliability of about 97.8% successful transmissions obtained under the simulated operating conditions.



Figure 6 Average WSN Latency Components

V. CONCLUSION

This investigation proposes a WSN-driven fault-localization framework for the 11 kV Trans-Amadi radial distribution feeders at Port Harcourt. The study addressed the issues relating to detection and location of faults in radial distribution systems. Fault-location data from the protection devices and physical inspection of the distribution line are normally inadequate in time and accuracy to be useful for locating the fault, especially when they are used to complement each other.

Mathematical models of the electrical parameters along the 11 kV Trans-Amadi distribution line were formulated based on the relationship between the line voltage drop and the three-phase current flows.

By simulating the 12-bus, 16.5 km radial distribution system, the voltage measured at the substation was found to reduce gradually from around 11.0 kV to 10.3 kV closer to the distribution-line terminal, while the branch current was observed to reduce incrementally downstream of the distribution system to cater for reduced power demand at the load end. These provide electrical system measurement parameters to facilitate WSN measurements and subsequent fault localization analysis. A distributed architecture was designed, built, and simulated by combining measurement vectors involving voltage, current, and phase-angle information from sensors for the WSN communications model. The simulation-based experiments showed that the volume of data acquired by the WSN increased with the sampling frequency: from below 2 kbps at 10 samples/s up to above 100 kbps at 1000 samples/s for three measurement channels with 16-bit resolution and 20% communication-overhead radio communication mode.

These data describe the relationship between electrical system measurement needs and WSN communication capacity.

The pilot algorithms designed for detection of abnormal system conditions and localization of faults could easily discriminate abnormal system states from normal by analyzing the normalized voltage and current deviations. The impedance-based algorithm was used to estimate the location of the fault from the changes in the measured phase angle deviations and complex impedance. The estimated faults location compared favorably with the real locations for the 10 simulated tests, the real locations being separated from the estimated locations by only 0.04 0.07 km.

© 2026 IJSRET

The evaluation of the performance of the algorithms for detecting and localization of faults showed that the typical detection times for the simulated measurement system were 16 and 24 ms while the typical communication latencies were 46 and 55 ms for the simulation-based algorithm for estimating the location of the fault. From a total of 200 cases of simulated faults, the average detection, communication, and processing times were 12.516.2 ms, 10.110.2 ms, and 11.811.0 ms, respectively, and the mean packet-delivery reliability was around 97.8%. The study therefore showed that the proposed mathematical framework could provide early distributed electrical system measurements and the fault-location estimates under the conditions simulated.

The study has created a clear roadmap for integrating the use of distributed measurement, wireless data communication, fault detection, and impedance-based method of estimating the location of faults along the distribution line.

The results, which are based on simulations, should not be taken as the actual measurement of the Trans-Amadi distribution system; the methodology should, therefore, incorporate measurements taken on field systems, the actual impedance data of the distribution systems, communication-channel characteristics, varying fault resistance, and practical measurement constraints to substantiate the simulation-based results.

REFERENCES

1. P. Baladuraikannan, *Power System Analysis: Short Circuit Studies*, lecture notes, VEMU Institute of Technology, Andhra Pradesh, India, 2023.
2. M. B. R. Widodo, O. Penangsang, A. S., and I. Suryawati, “Fault location detection using impedance and impulse injection on 20 kV distribution system based on geographic information system,” in *Proc. 4th Int. Conf. Software Eng. Inf. Manage.*, 2021, pp. 184–192.
3. M. K. Ngwenyama, P. F. Le Roux, and L. J. Ngoma, “Conventional method for electrical transmission system fault location detection,” in *Proc. 6th Asia Conf. Power Electr. Eng.*, 2021.
4. M. Jeevan, “A review on power system faults and protection,” *International Journal of Engineering Research & Technology*, vol. 11, no. 4, p. 395, 2022.
5. P. Stefanidou-Voziki, N. Sapountzoglou, B. Raison, and J. L. Dominguez-Garcia, “A review of fault location and classification methods in distribution grids,” *Electric Power Systems Research*, vol. 209, Art. no. 108031, 2022, doi: 10.1016/j.epsr.2022.108031.
6. M. Majidi, M. Etezadi-Amoli, and M. S. Fadali, “A novel method for single and simultaneous fault location in distribution networks,” *IEEE Transactions on Power Systems*, vol. 30, no. 6, pp. 3368–3376, 2015.
7. C. Ogomaka, K. Udofia, and N. Okpura, “Open-circuit fault detection for 11 kV distribution network using ANFIS,” *International Journal of Power Systems*, vol. 5, 2020.
8. A. H. A. Bakar, M. S. Ali, C. K. Tan, H. Mokhlis, H. Arof, and H. A. Illias, “High impedance fault location in 11 kV underground distribution systems using wavelet transforms,” *International Journal of Electrical Power & Energy Systems*, vol. 55, pp. 723–730, 2014, doi: 10.1016/j.ijepes.2013.10.003.
9. R. Orlowski, *Fault Detection and Location on 22 kV and 11 kV Distribution Feeders*, Ph.D. dissertation, Victoria University, Victoria, Australia, 2006.
10. M. Majidi and M. Etezadi-Amoli, “A new fault location technique in smart distribution networks using synchronized and nonsynchronized measurements,” *IEEE Transactions on Power Delivery*, vol. 33, no. 3, pp. 1358–1368, 2018.
11. A. Silos-Sanchez, R. Villafafila-Robles, and P. Lloret-Gallego, “Novel fault location algorithm for meshed distribution networks with DERs,” *Electric Power Systems Research*, vol. 181, Art. no. 106182, 2020, doi: 10.1016/j.epsr.2019.106182.
12. O. S. Rao, “Magnetic field around a current-carrying conductor,” *IOSR Journal of Applied Physics*, vol. 12, no. 3, pp. 46–49, 2020.
13. F. Loete, “A new insight on the ‘S’-shape pattern of soft faults in time-domain reflectometry,” *Group of Electrical Engineering Paris*, vol. 24, no. 23, 2023.
14. D. Albert *et al.*, “Power transformer hysteresis measurement,” in *Proc. 17th Symp. Energieinnovation*, 2022, pp. 1–11.
15. R. A. M. Mohamed, C. Gabrielli, J. S. Selker, F. Selker, S. C. Brooks, T. Ahmed, and K. C. Carroll, “Comparison of fibre-optic distributed temperature sensing and high-sensitivity sensor spatial surveying of stream temperature,” *Journal of Hydrology*, vol. 603, 2021.
16. V. A. Shneidman, *Electricity and Magnetism*, lecture notes for Phys. 121, Part II, Dept. Physics, New Jersey Institute of Technology, Newark, NJ, USA, 2025.
17. U. Pratiwi, G. A. Haddar, and M. Kristiawan, “Arduino-based mini reed switch magnetic sensor media: Implementation in physics learning to improve students’ analysing ability,” *Jurnal Iqra: Kajian Ilmu Pendidikan*, vol. 5, no. 1, pp. 183–193, 2020.

© 2026 IJSRET

18. G. V. Fernandez, *Magnetic Sensors: 2024 European School of Magnetism*, School of Physics, Engineering and Technology, University of York, York, U.K., 2024.
19. M. Kazim, A. H. Khawaja, U. Zabit, and Q. Huang, "Fault detection and localization for overhead 11 kV distribution lines with magnetic measurements," *IEEE Transactions on Instrumentation and Measurement*, vol. 69, no. 5, pp. 2028–2038, 2020.
20. X. Wang *et al.*, "Single-phase-to-ground fault location method of overhead line based on magnetic field detection and multi-criteria fusion," *International Journal of Electrical Power & Energy Systems*, vol. 145, Art. no. 108699, 2023, doi: 10.1016/j.ijepes.2022.108699.
21. S. M. Dehkordi, "Application of deep neural networks for load forecasting," in *Proc. 7th Int. Conf. Logistics and Supply Chain Management*, Tehran, Iran, 2020.
22. J. N. Emechebe, *Power System Analysis*, lecture notes, Dept. Electrical and Electronic Engineering, University of Abuja, Abuja, Nigeria, 2021.
23. Y. LeCun, Y. Bengio, and G. Hinton, "Deep learning," *Nature*, vol. 521, no. 7553, pp. 436–444, 2015, doi: 10.1038/nature14539.
24. P. Shrawane and T. S. Sidhu, "Performance of a noninvasive magnetic sensor-based current measurement system in power systems," *Electronics*, vol. 10, no. 22, Art. no. 2869, 2021.
25. A. F. Alqusayer and I. O. Habiballah, "Overview of single-line-to-ground fault analysis," *International Journal of Engineering Research & Technology*, vol. 11, no. 10, 2022.

© 2026 IJSRET